

**Update: Accurate determinations of  $\alpha_s$  from realistic lattice QCD**C. T. H. Davies,<sup>1</sup> K. Hornbostel,<sup>2</sup> I. D. Kendall,<sup>1</sup> G. P. Lepage,<sup>3,\*</sup> C. McNeile,<sup>1</sup> J. Shigemitsu,<sup>4</sup> and H. Trotter<sup>5</sup>

(HPQCD Collaboration)

<sup>1</sup>*Department of Physics and Astronomy, University of Glasgow, Glasgow G12 8QQ, United Kingdom*<sup>2</sup>*Southern Methodist University, Dallas, Texas 75275, USA*<sup>3</sup>*Laboratory for Elementary-Particle Physics, Cornell University, Ithaca, New York 14853, USA*<sup>4</sup>*Physics Department, The Ohio State University, Columbus, Ohio 43210, USA*<sup>5</sup>*Physics Department, Simon Fraser University, Vancouver, British Columbia, Canada*

(Received 15 September 2008; published 22 December 2008)

We use lattice QCD simulations, with MILC configurations (including vacuum polarization from  $u$ ,  $d$ , and  $s$  quarks), to update our previous determinations of the QCD coupling constant. Our new analysis uses results from 6 different lattice spacings and 12 different combinations of sea-quark masses to significantly reduce our previous errors. We also correct for finite-lattice-spacing errors in the scale setting, and for nonperturbative chiral corrections to the 22 short-distance quantities from which we extract the coupling. Our final result is  $\alpha_V(7.5 \text{ GeV}, n_f = 3) = 0.2120(28)$ , which is equivalent to  $\alpha_{\overline{\text{MS}}}(M_Z, n_f = 5) = 0.1183(8)$ . We compare this with our previous result from Wilson loops, which differs by one standard deviation.

DOI: [10.1103/PhysRevD.78.114507](https://doi.org/10.1103/PhysRevD.78.114507)

PACS numbers: 11.15.Ha, 12.38.Aw, 12.38.Gc

**I. INTRODUCTION**

An accurate value for the coupling constant  $\alpha_s$  in quantum chromodynamics (QCD) is important both for QCD phenomenology and as an input for possible theories beyond the standard model. Some of the most accurate values for the coupling constant come from numerical simulations of QCD using lattice techniques, when combined with very accurate experimental data for hadron masses. In this paper we update our previous determinations of the coupling from Wilson loops in lattice QCD [1]. Our new analysis takes advantage of new simulation results, from the MILC collaboration, that employ smaller lattice spacings  $a$ . We also now account systematically for chiral corrections associated with the masses of sea quarks in the simulation, and for  $\mathcal{O}(a^n)$  uncertainties in the values we use for the lattice spacing.

Few-percent accurate QCD simulations have only become possible in the last few years, with the development of much more efficient techniques for simulating the sea quarks; see, for example, [2] for an overview and references. The simulations we use include only light quarks ( $u$ ,  $d$ , and  $s$ ) in the vacuum polarization; the effects of  $c$  and  $b$  quarks are incorporated using perturbation theory, which is possible because of their large masses. Our lattice QCD analysis proceeds in two steps. First the QCD parameters—the bare coupling constant and bare quark masses in the Lagrangian—must be tuned. For each value of the bare coupling, we set the lattice spacing to reproduce the correct  $Y' - Y$  meson mass difference in the simulations,

while we tune the  $u/d$ ,  $s$ ,  $c$ , and  $b$  masses to give correct values for  $m_\pi^2$ ,  $2m_K^2 - m_\pi^2$ ,  $m_{\eta_c}$ , and  $m_Y$ , respectively; more information can be found in [2]. For efficiency we set  $m_u = m_d$ ; this leads to negligible errors in the analysis presented here. Once these parameters are set, there are no further physics parameters, and the simulation will accurately reproduce QCD.

Having an accurately tuned simulation of QCD, we use it to compute nonperturbative values for a variety of short-distance quantities, each of which has a perturbative expansion of the form

$$Y = \sum_{n=1}^{\infty} c_n \alpha_V^n(d/a), \quad (1)$$

where  $c_n$  and  $d$  are dimensionless  $a$ -independent constants, and  $\alpha_V(d/a)$  is the (running) QCD coupling constant, with  $n_f = 3$  light-quark flavors, in the  $V$  scheme [3,4]. Given the coefficients  $c_n$ , which are computed using Feynman diagrams, we choose  $\alpha_V(d/a)$  so that the perturbative formula for  $Y$  reproduces the nonperturbative value given by the simulation. Given  $d$  and  $a$ , and the  $c$  and  $b$  masses, we can then use perturbation theory to convert  $\alpha_V(d/a)$  to the more conventional coupling constant  $\alpha_{\overline{\text{MS}}}(M_Z, n_f = 5)$ , evaluated at the mass of the  $Z$  meson [5,6].

This analysis is complicated by nonperturbative contributions to  $Y$  and by simulation uncertainties in the value of the lattice spacing  $a$ , which enters Eq. (1). It is also complicated by perturbative uncertainties. We know the values of the coefficients  $c_n$  through order  $n = 3$  (next-to-next-to-leading order) for the quantities we examine, yet unknown higher-order coefficients still have an impact at

\*g.p.lepage@cornell.edu

the level of accuracy we seek. A main focus of this paper is to address these complications and quantify the uncertainties in our determination of the coupling constant. In Sec. II we review the perturbative expansions for our short-distance quantities, all but one of which are derived from small Wilson loops [7]. The Monte Carlo simulation results for these loops are presented in Sec. III. We discuss finite-lattice-spacing errors and chiral corrections in Sec. IV. In Sec. V, we describe how we combine perturbation theory with simulation results using constrained (Bayesian) fitting methods. There we present our results and discuss in detail the various uncertainties that arise. Finally, in Sec. VI, we summarize our results.

## II. PERTURBATION THEORY

The simplest short-distance quantities to simulate are vacuum expectation values of Wilson loop operators:

$$W_{mn} \equiv \frac{1}{3} \langle 0 | \text{Re Tr Pe}^{-ig \oint_{nm} A \cdot dx} | 0 \rangle, \quad (2)$$

where P denotes path ordering,  $A_\mu$  is the QCD vector potential, and the integral is over a closed  $ma \times na$  rectangular path. Wilson loops should be calculable in (lattice QCD) perturbation theory when  $ma$  and  $na$  are small. We computed perturbative coefficients through order  $n = 3$  for

six small, rectangular loops, and also for two nonplanar paths:

$$\text{BR} = \begin{array}{c} \text{---} \rightarrow \\ \uparrow \\ \text{---} \rightarrow \\ \downarrow \\ \text{---} \rightarrow \end{array} \quad \text{CC} = \begin{array}{c} \text{---} \rightarrow \\ \uparrow \\ \text{---} \rightarrow \\ \downarrow \\ \text{---} \rightarrow \end{array} . \quad (3)$$

The coefficients for our various loops are derived in [8]. The results are for the gluon and quark actions used to create the MILC gluon-configuration sets used in this study. They also assume  $n_f = 3$  massless sea quarks. The quarks in our simulations are not exactly massless, but the masses are sufficiently small that the difference is negligible,  $\mathcal{O}(\alpha_V^2(am)^2)$ , in perturbation theory (but less so nonperturbatively, as we will discuss).

Perturbation theory is more convergent for the logarithm of a Wilson loop than it is for the loop itself. This is because the perturbative expansion of a loop is dominated by a self-energy contribution that is proportional to the length of the loop, and this contribution exponentiates for large loops. The length of the loop factors out of the expansion when we take the logarithm. This structure is evident in Table I where we tabulate the perturbative coefficients for the logarithms of our loops. The renormalization scales  $d/a$  for each quantity are determined using the procedures described in [3,4,9].

TABLE I. Perturbative scale and coefficients for several small Wilson loops  $W_{ij}$ , Creutz ratios, tadpole-improved Wilson loops, and the tadpole-improved bare coupling  $\alpha_{\text{lat}}/W_{11}$ . Parameters  $d$  and  $c_i$  are defined in Eq. (1). Coefficients  $c_1, c_2, c_3$  are from lattice perturbation theory; coefficients  $c_4, c_5$  are from the fits to results from multiple lattice spacings described in this paper. These results are for the  $a^2$ -improved gluon action used by the MILC collaboration, with the ASQTAD action for vacuum polarization from  $n_f = 3$  massless quarks. Similar types of short-distance quantity are grouped.

	$d$	$c_1$	$c_2/c_1$	$c_3/c_1$	$c_4/c_1$	$c_5/c_1$
$-\log W_{11}$	3.325	3.068 40	-1.0683 (2)	1.70 (4)	-4 (2)	-0 (4)
$-\log W_{12}$	2.998	5.551 20	-0.8585 (4)	1.72 (4)	-4 (2)	-1 (4)
$-\log W_{\text{BR}}$	3.221	4.834 25	-0.8547 (3)	1.80 (4)	-4 (2)	-1 (4)
$-\log W_{\text{CC}}$	3.047	5.297 58	-0.7941 (3)	1.86 (4)	-4 (2)	-1 (5)
$-\log W_{13}$	2.934	7.876 56	-0.7437 (8)	1.75 (5)	-4 (2)	-1 (4)
$-\log W_{14}$	2.895	10.171 58	-0.6870 (8)	1.70 (6)	-4 (2)	-1 (4)
$-\log W_{22}$	2.582	9.199 70	-0.6923 (10)	1.86 (5)	-4 (2)	-1 (4)
$-\log W_{23}$	2.481	12.342 82	-0.5995 (13)	2.00 (6)	-4 (2)	-1 (5)
$-\log W_{13}/W_{22}$	2.397	-1.323 13	0.5969 (84)	1.11 (21)	-2 (2)	-1 (3)
$-\log W_{11} W_{22}/W_{12}^2$	2.169	1.165 69	0.7361 (86)	1.21 (22)	-4 (2)	-1 (3)
$-\log W_{\text{CC}} W_{\text{BR}}/W_{11}^3$	2.728	0.926 65	2.2825 (19)	0.78 (9)	-4 (2)	-2 (6)
$-\log W_{\text{CC}}/W_{\text{BR}}$	2.730	0.463 33	0.5103 (35)	1.16 (12)	-2 (2)	-1 (3)
$-\log W_{14}/W_{23}$	2.066	-2.171 24	0.5838 (84)	1.83 (29)	-3 (3)	-1 (4)
$-\log W_{11} W_{23}/W_{12} W_{13}$	1.970	1.983 45	0.7062 (88)	1.64 (27)	-3 (3)	-1 (4)
$-\log W_{12}/u_0^6$	2.470	0.948 61	0.6011 (19)	0.05 (8)	-3 (2)	-1 (2)
$-\log W_{\text{BR}}/u_0^6$	2.720	0.231 66	4.0516 (41)	0.36 (16)	-8 (6)	-3 (10)
$-\log W_{\text{CC}}/u_0^6$	2.730	0.694 99	1.6925 (20)	0.91 (8)	-3 (3)	-1 (4)
$-\log W_{13}/u_0^8$	1.888	1.739 77	0.4019 (34)	-0.44 (10)	-2 (1)	-1 (2)
$-\log W_{14}/u_0^{10}$	1.892	2.500 59	0.4817 (33)	-0.68 (15)	-2 (1)	-1 (2)
$-\log W_{22}/u_0^8$	2.290	3.062 91	0.6149 (30)	0.44 (9)	-2 (2)	-1 (2)
$-\log W_{23}/u_0^{10}$	2.030	4.671 83	0.5714 (35)	0.55 (11)	-2 (2)	-1 (2)
$\alpha_{\text{lat}}/W_{11}$	3.325	1.000 00	-0.4212 (2)	0.72 (4)	-4 (1)	-1 (2)

The perturbative coefficients in  $\log(W)$ , while greatly reduced by the logarithm, are still rather large. They can be further reduced in two ways. One is to ‘‘tadpole improve’’  $W_{mn}$  by dividing by  $u_0^{2(n+m)}$  where [3]

$$u_0 \equiv (W_{11})^{1/4}. \quad (4)$$

The other is to examine Creutz ratios of the loops rather than the loops themselves [3]. Each procedure significantly reduces the known high-order coefficients, as is clear in Table I. We use seven tadpole-improved loops and six Creutz ratios in our analysis. Each has smaller  $\alpha_V^3$  coefficients, which improves convergence, but each also has a significantly smaller scale  $d/a$ , which slows convergence (since  $\alpha_V(d/a)$  is larger).

We also include in Table I the perturbative expansion for the tadpole-improved bare coupling constant,  $\alpha_{\text{lat}}/W_{11}$ , where  $\alpha_{\text{lat}}$  is the coupling constant that appears in the gluon action for a given lattice spacing [3]. This is another, independent, short-distance quantity from which  $\alpha_V$  can be determined.

We used Feynman diagrams to compute perturbative coefficients  $c_n$  for  $n \leq 3$ . Higher-order coefficients can be estimated by simultaneously fitting results from different lattice spacings to the same perturbative formula [1]. This is possible because the coupling  $\alpha_V(d/a)$  changes value with different lattice spacings  $a$ :

$$q^2 \frac{d\alpha_V(q)}{dq^2} = -\beta_0 \alpha_V^2 - \beta_1 \alpha_V^3 - \beta_2 \alpha_V^4 - \beta_3 \alpha_V^5, \quad (5)$$

where the  $\beta_i$  are constants [6]. In this paper, we follow our earlier analysis by parametrizing the running coupling by its value at 7.5 GeV,

$$\alpha_0 \equiv \alpha_V(7.5 \text{ GeV}, n_f = 3). \quad (6)$$

Given  $\alpha_0$ , the coupling at any other scale can be obtained by integrating Eq. (5) (which we do numerically).

For the purposes of this paper, we define  $\alpha_V$  in fourth order and beyond so that the evolution equation, Eq. (5), is exact, with no higher-order terms beyond  $\beta_3$ . This definition gives precise meaning to the perturbative coefficients  $c_n$  for  $n \geq 4$  that we determine by fitting the  $a$ -dependence of our short-distance quantities [10].

Our main result is a value for  $\alpha_0$ . To facilitate comparisons with other analyses, we convert this result to the  $\overline{\text{MS}}$  scheme [6], add in  $c$  and  $b$  vacuum polarization perturbatively [5], and then evolve to the mass of the  $Z$  meson, again using perturbation theory [6].

### III. QCD SIMULATIONS

The gluon-configuration sets we use were created by the MILC collaboration [11]. The relevant simulation parameters are listed in Table II.

The input parameters for a QCD simulation are the bare coupling constant and bare quark masses. The coupling constant is specified through the  $\beta$  parameter, listed in Table II, where

$$\alpha_{\text{lat}} \equiv \frac{5}{2\pi\beta}. \quad (7)$$

The bare quark masses,  $m_{0\ell}(a)$  for  $u/d$  quarks and  $m_{0s}(a)$  for  $s$  quarks, used in the simulations are also listed, in units of the lattice spacing and, following MILC conventions, multiplied by  $u_0$  [Eq. (4)]. The bare masses corresponding to fixed physical masses (of, for example, pions) vary with the lattice spacing. To facilitate comparisons between lattice spacings, we use first-order perturbation theory to evolve all of our masses to a common value for the lattice spacing, which we take to be the smallest lattice spacing in

TABLE II. QCD parameters for the 12 different sets of gluon configurations used in this paper [11]. Parameter  $\beta$  specifies the bare coupling constant. The inverse lattice spacing is specified in terms of the  $r_1$ , and the bare quark masses are in units of the lattice spacing and multiplied by  $u_0$ . The spatial and temporal sizes,  $L$  and  $T$ , are also given. Configuration sets that were tuned to have the same lattice spacing are grouped.

Set	$\beta$	$r_1/a$	$au_0m_{0\ell}$	$au_0m_{0s}$	$L/a$	$T/a$
1	6.458	1.802(10)	0.0082	0.082	16	48
2	6.572	2.133(14)	0.0097	0.0484	16	48
3	6.586	2.129(12)	0.0194	0.0484	16	48
4	6.76	2.632(13)	0.005	0.05	24	64
5	6.76	2.610(12)	0.01	0.05	20	64
6	6.79	2.650(08)	0.02	0.05	20	64
7	7.09	3.684(12)	0.0062	0.031	28	96
8	7.11	3.711(13)	0.0124	0.031	28	96
9	7.46	5.264(13)	0.0018	0.018	64	144
10	7.47	5.277(16)	0.0036	0.018	48	144
11	7.48	5.262(22)	0.0072	0.018	48	144
12	7.81	7.127(34)	0.0028	0.014	64	192

TABLE III. Simulation results for the vacuum expectation values of various small Wilson loops. Results are given for each of the 12 different configuration sets in Table II.

Set	$W_{11}$	$W_{12}$	$W_{13}$	$W_{14}$	$W_{22}$	$W_{23}$	$W_{BR}$	$W_{CC}$
1	0.534 101(17)	0.280 720(22)	0.149 263(21)	0.079 710(19)	0.087 438(23)	0.030 150(16)	0.338 982(22)	0.287 376(25)
2	0.548 012(51)	0.298 624(68)	0.165 063(67)	0.091 701(63)	0.101 572(73)	0.038 333(54)	0.356 763(68)	0.306 315(78)
3	0.549 470(53)	0.300 310(70)	0.166 530(70)	0.092 797(63)	0.102 640(76)	0.039 007(54)	0.358 570(70)	0.308 140(79)
4	0.567 069(16)	0.323 163(21)	0.187 281(24)	0.109 122(27)	0.121 542(19)	0.050 751(15)	0.381 148(25)	0.332 184(27)
5	0.566 961(21)	0.322 987(27)	0.187 084(26)	0.108 927(21)	0.121 341(29)	0.050 579(21)	0.380 988(26)	0.331 996(29)
6	0.569 716(21)	0.326 496(27)	0.190 278(26)	0.111 479(21)	0.124 204(29)	0.052 397(21)	0.384 479(26)	0.335 685(29)
7	0.594 843(7)	0.359 761(9)	0.221 624(10)	0.137 271(10)	0.153 433(12)	0.072 261(10)	0.417 002(9)	0.370 239(10)
8	0.596 408(12)	0.361 838(19)	0.223 616(17)	0.138 946(16)	0.155 315(18)	0.073 593(16)	0.419 020(16)	0.372 372(17)
9	0.620 813(5)	0.394 837(8)	0.255 897(9)	0.166 723(9)	0.186 116(7)	0.096 208(6)	0.450 947(7)	0.406 300(8)
10	0.621 462(3)	0.395 717(4)	0.256 770(5)	0.167 486(5)	0.186 959(5)	0.096 852(5)	0.451 798(4)	0.407 210(5)
11	0.622 115(2)	0.396 607(4)	0.257 650(4)	0.168 257(4)	0.187 809(5)	0.097 491(4)	0.452 654(3)	0.408 123(4)
12	0.641 947(2)	0.423 992(3)	0.285 304(5)	0.192 943(5)	0.214 759(4)	0.118 532(3)	0.478 903(3)	0.436 064(4)

our analysis:

$$m_q \equiv m_{0q}(a_{\min}). \quad (8)$$

The  $s$ -quark masses here are approximately correct. The  $u/d$  masses are generally too large, but small enough to allow accurate extrapolations to the correct values.

The lattice spacing is not an input to QCD simulations. Rather it is extracted from calculations of physical quantities in the simulation. Here we use MILC's determinations of  $r_1/a$  for this purpose, where  $r_1$  is defined in terms of the static-quark potential [11]. The values for each configuration set are listed in Table II. To obtain the lattice spacing, we need to know  $r_1$ . We use the value,  $r_1 = 0.321(5)$  fm, determined from simulation results for the  $Y' - Y$  mass splitting [12]. The uncertainties quoted for  $r_1/a$  in Table II are predominantly statistical; they do not include potential errors due to the finite lattice spacing or mistuned light-quark masses, which we will discuss later.

The lattices we use here have lattice spacings that range from 0.18 fm to 0.045 fm. The spatial volumes are 2.4 fm across or larger in each case.

Our simulation results for the vacuum expectations of our 8 different Wilson loops, each for each of our 12 different configuration sets, are presented in Table III. The uncertainties quoted are statistical. Step-size errors, due to the algorithm used to generate gluon configurations, are no larger than the statistical errors [13] and therefore, like statistical errors, are negligible; we will ignore them here.

#### IV. SYSTEMATIC ERRORS

The goal of our analysis is to determine  $\alpha_0 \equiv \alpha_V(7.5 \text{ GeV})$ . The only relevant systematic errors, other than from the truncation of perturbation theory, are from nonperturbative effects and from  $a^2$  errors in our determination of the lattice spacings. Finite-volume errors are no

larger than our statistical errors, as we have verified by examining configuration set 5 with  $L/a = 28$  in addition to  $L/a = 20$ . Statistical errors are also negligible (and therefore we ignored statistical correlations between different Wilson loops when computing Creutz ratios, whose real statistical errors are 2–3 times smaller than what we use here). We consider each systematic effect in term.

#### A. Chiral corrections

Wilson loops, being very short distance, are almost independent of the light-quark masses. The dependence in perturbation theory is  $\mathcal{O}(\alpha_V^2(am_q)^2)$ , which is negligible here given other errors. There is a larger contribution, however, from nonperturbative contributions that is important to our analysis. This contribution can be parametrized using chiral perturbation theory and the operator product expansion, which says that an arbitrary QCD operator  $O_{\text{QCD}}$  that is local at scale  $\Lambda$  can be expanded in terms of local operators  $O_n$  from the chiral theory:

$$O_{\text{QCD}} \equiv \sum_n b_n \frac{O_n}{\Lambda^{d_n}}, \quad (9)$$

where  $d_n$  is the dimension of  $O_n$  minus the dimension of  $O_{\text{QCD}}$ . Here equivalence between the left-hand and right-hand sides means that matrix elements of the operators are equal for comparable physical states in QCD and the chiral theory.

For Wilson loops, we are interested in vacuum expectation values and singlet operators. The scale  $\Lambda$  for a loop of size  $L$  is  $\Lambda \sim 1/L$ . Consequently, we expect

$$W \equiv b_0 + b_1 L \text{Tr}(m(U + U^\dagger)) + b_2 L^2 \text{Tr}(\partial_\mu U \partial^\mu U^\dagger) + \dots, \quad (10)$$

where  $m = \text{diag}(m_u, m_d, m_s)$  breaks chiral symmetry, and  $U \equiv \exp(i\phi/F)$  with

$$\phi = \phi^\dagger \equiv \begin{bmatrix} \pi^0/\sqrt{2} + \eta_8/\sqrt{6} & \pi^+ & K^+ \\ \pi^- & -\pi^0/\sqrt{2} + \eta_8/\sqrt{6} & K^0 \\ K^- & \bar{K}^0 & -2\eta_8/\sqrt{6} \end{bmatrix} \quad (11)$$

and  $F \approx 92$  MeV.

Taking the vacuum expectation value and a logarithm, and keeping only the leading  $\mathcal{O}(a)$  terms, we get

$$\begin{aligned} \log\langle W \rangle &\approx w^{(0)}(1 + w_m^{(1)} a(\text{Tr}(m(U + U^\dagger))) \\ &\approx w^{(0)}(1 + w_m^{(1)} a(2m_l + m_s) + \dots). \end{aligned} \quad (12)$$

Standard methods can be used to compute higher-order corrections, including chiral logarithms, from the expansion of  $\text{Tr}(m(U + U^\dagger))$ , but these are too small to be relevant to our analysis.

The leading contribution,  $w^{(0)}$ , is obtained from the perturbative analysis discussed in Sec. II, provided the loops are sufficiently small to be perturbative. We expect  $w_m^{(1)}$  to be roughly independent of loop size since  $w^{(0)}$  is approximately proportional to  $L/a$  (see Sec. II).

We can estimate the size of  $w_m^{(1)}$  from a simple argument. For light-quark hadrons, hadronic quantities like meson decay constants or baryon masses depend approximately linearly on the masses of their valence quarks. The mass  $m_v$  of a valence quark makes a contribution of order  $Qm_v/\Lambda$  to some hadronic quantity  $Q$ , where  $\Lambda$  is a momentum scale characteristic of the size of the hadron ( $\approx$  the chiral scale, for light-quark hadrons). From ratios of decay constants like  $f_K/f_\pi$  or of baryon masses like  $m(\Lambda^0)/m(p^+)$ , it is clear that  $m_s/\Lambda$  is of order 20%, and therefore that  $\Lambda \approx 400$  MeV. Empirically contributions from individual sea-quark masses are 3–5 times smaller than those from individual valence-quark masses [14]. Consequently, the relative contribution from a sea-quark mass  $m_q$  should be roughly  $m_q/1.2$  GeV.

Now consider Wilson loops. The  $m_q$  dependence of  $\log(W_{11})$ , for example, should be much smaller than that for a light-quark hadron because the loop is much smaller than the hadron. The typical radius of such hadrons is around 1 fm, so we expect the relative contribution to  $W_{11}$  from a sea-quark mass of  $m_q$  to be approximately

$$\frac{a}{1 \text{ fm}} \frac{m_q}{1.2 \text{ GeV}} \approx \frac{am_q}{6}. \quad (13)$$

Therefore we expect  $w_m^{(1)} = \mathcal{O}(1/6)$ . This implies corrections to our  $\log(W)$ s, for example, of order 1%–2% on the coarsest lattices and 0.3%–0.5% on the finest lattices—which is large compared with the statistical errors in these quantities, and therefore important.

In most lattice calculations we want the light-quark masses as close to their physical values as possible, so that lattice results reproduce what is seen in experiments. The situation for our Wilson loops is different, however. In our simulations here we are trying to isolate the perturba-

tive part of the loop, in order to compare it with perturbation theory (not experiment), and the linear quark-mass dependence is a nonperturbative contamination that we want to remove. Consequently, the precise values of the quark masses are not relevant so long as they are small enough that we can correct for them (or ignore them), which is the case here.

## B. Gluon condensate

The leading gluonic nonperturbative contribution comes from the gluonic condensate,  $\langle \alpha_s G^2/\pi \rangle$ . The contribution of the condensate to a Wilson loop is easily calculated to leading order in perturbation theory:

$$\delta W_{\text{cond}} = -\frac{\pi^2}{36} \left(\frac{A}{a^2}\right)^2 a^4 \langle \alpha_s G^2/\pi \rangle, \quad (14)$$

where  $A$  is the loop area for planar loops. We remove this contribution from our Wilson loops before comparing them with perturbation theory. The value of the condensate is not well known, so we take  $\langle \alpha_s G^2/\pi \rangle = 0.0 \pm 0.012$  GeV<sup>4</sup>, which covers the range of expectations [15]. We also allow for higher-dimension condensate contributions by replacing

$$\delta W_{\text{cond}} \rightarrow \delta W_{\text{cond}}(1 + w_{\text{cond}}^{(2)}(a\Lambda_g)^2 + w_{\text{cond}}^{(4)}(a\Lambda_g)^4 + \dots), \quad (15)$$

where we take  $\Lambda_g = 1$  GeV and coefficients  $w_{\text{cond}}^{(i)} = 0 \pm 1$ . To be certain that we do not underestimate errors we include 10 condensate terms in all [16].

We chose the number of condensate terms here somewhat arbitrarily. Only results from the largest loops are affected appreciably even by the leading-order condensate correction, and then only by amounts of order a standard deviation in our final results for the coupling. While a leading-order condensate value of 0.006, for example, shifts  $\log W_{23}$  by about 25% for our largest lattice spacings, the shift is less than 0.1% for the smallest lattice spacing, which is more important in our analysis. Smaller loops are much less sensitive: for example, this gluon condensate shifts  $\log W_{11}$  by only 0.3% for the largest lattice spacings, and by only 0.003% for the smallest lattice spacings. The two Creutz ratios that involve  $W_{23}$  are the most sensitive to condensate contributions, but even they are shifted by only 0.2%–0.25% for the smallest lattice spacings [17].

## C. Finite- $a$ errors

In our analysis, the scale for the couplings comes from the lattice spacing, and the lattice spacing comes from measurements of  $r_1/a$  in the simulations. As for any

physical quantity, lattice QCD measurements of  $r_1$  have finite- $a$  errors; and, using an analysis similar to the one we outlined for Wilson loops, they should also be approximately linear in the sea-quark masses. Consequently, we expect

$$r_1^{\text{lat}} = r_1(1 + r_{1a}^{(2)}(a/r_1)^2 + r_{1m}^{(1)}r_1(2\delta m_l + \delta m_s) + \dots), \quad (16)$$

where  $r_{1a}^{(2)} = \mathcal{O}(\alpha_s \approx 1/3)$  [18], since the gluon action has no tree-level errors in  $\mathcal{O}(a^2)$ ; and  $r_{1m}^{(1)} = \mathcal{O}(1/6)$ , following the discussion for Wilson loops. Here  $\delta m_q$  is the simulation's tuning error in the mass for sea-quark  $q$  —  $\delta m_l \approx m_l$  for our simulations, while  $\delta m_s \approx 0$ . These corrections could affect our lattice spacings by as much as several percent, although the impact on  $\alpha_0$  is suppressed by a power of  $\alpha_0$  and so is much less. We allow for both corrections in our analysis.

## V. ANALYSIS AND RESULTS

We have 22 different short-distance quantities in our analysis, each of which produces a separate value for  $\alpha_0 \equiv \alpha_V(7.5 \text{ GeV})$ . These consist of  $\log(W)$ s for each of 8 Wilson loops, 6 independent Creutz ratios built from these loops, 7 tadpole-improved  $\log(W)$ s, and the tadpole-improved bare coupling  $\alpha_{\text{lat}}/W_{11}$ . We have 12 values for each of these quantities, with one for each configuration set in Table II. In this section we discuss first the fitting method used for extracting  $\alpha_0$ , and then we review our results.

### A. Constrained fits

We analyze each short-distance quantity  $Y$  separately. We use a constrained fitting procedure, based upon Bayesian ideas [19], to fit the values  $Y_i \pm \sigma_{Y_i}$  coming from each of our configuration sets (Table III) to a single formula. In this procedure we minimize an augmented  $\chi^2$  function of the form

$$\chi^2 \equiv \sum_{i=1}^{12} \frac{(Y_i - Y(a_i, (am_q)_i, \alpha_0, y_m^{(1)}, c_n, d))^2}{\sigma_{Y_i}^2} + \sum_{\xi} \delta\chi_{\xi}^2, \quad (17)$$

where  $i$  labels the configuration set, and

$$\begin{aligned} & Y(a_i, (am_q)_i, \alpha_0, y_m^{(1)}, c_n, d) \\ &= (1 + y_m^{(1)}(2am_l + am_s)_i) \sum_{n=1}^{10} c_n \alpha_V^n(d/a_i). \end{aligned} \quad (18)$$

The sea-quark mass dependence here is from Eq. (12). The lattice spacing in each case is determined from the simulation values for  $(r_1/a)_i$  from each configuration set (Table II) using

$$a_i = \frac{r_1}{(r_1/a)_i} (1 + r_{1a}^{(2)}(a/r_1)_i^2 + r_{1m}^{(1)}(2r_1 m_l)_i), \quad (19)$$

which follows from Eq. (16), taking  $\delta m_l \approx m_l$  and  $\delta m_s \approx 0$ , and  $r_1 = 0.321(5) \text{ fm}$  [12]. Here  $(r_1 m_q)_i \equiv (am_q)_i \times (r_1/a)_i$ . Given the lattice spacing, the coupling  $\alpha_V(d/a)$  is computed from  $\alpha_0$  by integrating Eq. (5) numerically.

The  $\chi^2$  function is minimized by varying fit parameters like the  $c_n$  (but not  $d$  which is effectively exact). Every fit parameter in our procedure is constrained by an extra term or “prior”  $\delta\chi_{\xi}^2$  in the  $\chi^2$  function. The expansion parameters  $c_n$  from perturbation theory, for example, are constrained by

$$\delta\chi_{c_n}^2 = \sum_{n=1}^{10} \frac{(c_n - \bar{c}_n)^2}{\sigma_{c_n}^2}, \quad (20)$$

which implies that the fit will explore values for  $c_n$  that are centered around  $\bar{c}_n$  with a range specified by  $\sigma_{c_n}$ :  $\bar{c}_n \pm \sigma_{c_n}$ . For  $n \leq 3$ , we set  $\bar{c}_n$  to the value obtained from our numerical evaluation of the relevant Feynman diagrams, with  $\sigma_{c_n}$  equal to the uncertainty in that evaluation. For  $n \geq 4$ , we set  $\bar{c}_n = 0$  and

$$\sigma_{c_n} = 2.5 \max(|c_1|, |c_2|, |c_3|). \quad (21)$$

Thus the  $c_n$ s in the fit are constrained by the values obtained from our Feynman integrals where these are available (taking correct account of the uncertainties in those values), while the others are allowed to vary over a range that is 2.5 times larger than the largest known coefficient. The factor 2.5 was chosen using the empirical Bayes criterion, described in [19], applied to the  $\log(W)$ s; applying the same criterion to the other quantities would have given smaller factors, but we take the more conservative factor of 2.5 for these as well.

We include seven  $c_n$ s beyond the ones currently known from perturbation theory to illustrate an important issue. In reality there are infinitely many  $c_n$ s, but in practice the various uncertainties in our analysis mean that it is sensitive only to the first few. As we add  $c_n$ s the fit improves but only up to a point— $n = 4$  for  $\log(W)$ s. As long as priors are included in  $\chi^2$ , terms can be added beyond this point but they have no effect on the result of the fit (including the error estimate) or on the quality of the fit. We add terms through  $n = 10$  to be certain we have reached this point. Our analysis is not sufficiently accurate to yield new information about  $c_n$ s with  $n > 4$  (beyond what is incorporated in the prior); but, by adding enough  $c_n$ s so that the fit results and errors cease changing, we guarantee that our final error estimates include the full uncertainty due to the fact that we have *a priori* values for only a few of the coefficients.

Other fit parameters, like  $\alpha_0$ ,  $y_m^{(1)}$ ,  $r_{1a}^{(2)}$ , and  $r_{1m}^{(1)}$  must also have priors:

$$\delta\chi_0^2 = \frac{(\log(\alpha_0) - \overline{\log(\alpha_0)})^2}{\sigma_{\log(\alpha_0)}^2} + \frac{(y_m^{(1)} - \bar{y}_m^{(1)})^2}{\sigma_{y_m^{(1)}}^2} + \frac{(r_{1a}^{(2)} - \bar{r}_{1a}^{(2)})^2}{\sigma_{r_{1a}^{(2)}}^2} + \frac{(r_{1m}^{(1)} - \bar{r}_{1m}^{(1)})^2}{\sigma_{r_{1m}^{(1)}}^2}. \quad (22)$$

We constrain  $\log(\alpha_0)$  to be  $-1.6 \pm 0.5$ ; this prior has negligible effect on the fits because it is so broad (and the fits are so sensitive to  $\alpha_0$ ). Following the discussion in Sec. IV, we set

$$\bar{y}_m^{(1)} = \bar{r}_{1m}^{(1)} = 0, \quad \sigma_{y_m^{(1)}} = \sigma_{r_{1m}^{(1)}} = 1/6. \quad (23)$$

We checked the width of these two priors using the empirical Bayes criterion and found that, in fact, this is the optimal width indicated by our simulation results. For  $r_{1a}^{(2)}$ , the empirical Bayes criterion suggests a width for the prior that is twice what we anticipated in Sec. IV C:

$$\bar{r}_{1a}^{(2)} = 0, \quad \sigma_{r_{1a}^{(2)}} = 2\alpha_s \approx 0.6. \quad (24)$$

We use this more conservative prior in our fits. Higher-order corrections are easily added but have no impact because the corrections are too small to matter, given the size of our other errors.

Our simulation result for  $(r_1/a)_i$ , which is used to determine the lattice spacing  $a_i$  for the  $i$ th configuration set [Eq. (19)], is not exact. To include its uncertainty in our analysis we treat  $(r_1/a)_i$  as a fit parameter, to be varied while minimizing  $\chi^2$ , but with a prior whose mean is the value measured in the simulation and whose width is the measured uncertainty (as in Table II). We can incorporate the uncertainty in the value of  $r_1$  using the same trick, with  $r_1$  as a fit parameter:

$$\delta\chi_{r_1}^2 = \frac{(r_1 - \bar{r}_1)^2}{\sigma_{r_1}^2} + \sum_{i=1}^{12} \frac{((r_1/a)_i - \overline{(r_1/a)_i})^2}{\sigma_{(r_1/a)_i}^2}, \quad (25)$$

where  $\bar{r}_1 \pm \sigma_{r_1} = 0.321 \pm 0.005$  fm [12].

The  $c$  and  $b$  masses are required to convert  $\alpha_0$  to  $\alpha_{\overline{\text{MS}}}(M_Z, n_f = 5)$ . We account for the uncertainties in these masses by including them as fit parameters, with appropriate priors, together with fit parameters for unknown high-order terms in the  $\overline{\text{MS}}$   $\beta$ -function, and in the perturbative formulas for incorporating  $c$  and  $b$  vacuum polarization [5,6]. For the  $\beta$ -function, we allow for a sixth-order term  $\beta_4 \alpha_{\overline{\text{MS}}}^6$  in the evolution equation [analogous to Eq. (5) for  $\alpha_V$ ] where  $\beta_4$  is a fit parameter with a prior centered on  $\bar{\beta}_4 = 0$  with width

$$\sigma_{\beta_4} = \max(|\beta_0|, |\beta_1|, |\beta_2|, |\beta_3|) \quad (26)$$

for the  $\overline{\text{MS}}$   $\beta_i$ s. We include analogous corrections, fit parameters, and priors for the formulas for  $c$  and  $b$  vacuum polarization.

## B. Results

The results from our 22 determinations of the coupling are listed and shown in Fig. 1. The gray band corresponds to our final result of

$$\alpha_{\overline{\text{MS}}}(M_Z, n_f = 5) = 0.1183(8), \quad (27)$$

which was obtained from a weighted average of all of 22 determinations [20]. Our error estimate here is that of a typical entry in the plot; combining our results does not reduce errors because most of the uncertainty in each result is systematic. The individual results in the plot are consistent with each other:  $\chi^2/22 = 0.2$  for the 22 entries in Fig. 1. And the fits for each quantity separately are excellent as well:  $\chi^2/12 = 0.3$  to  $0.6$  for our fits to the 12 pieces of simulation data (one from each configuration set) for each quantity. The results in Fig. 1 are derived, using perturbation theory (Sec. II), from the fit values for  $\alpha_0$ , which average to

$$\alpha_0 = \alpha_V(7.5 \text{ GeV}, n_f = 3) = 0.2120(28), \quad (28)$$

where again the error is that of a typical result for a single short-distance quantity (it is *not* reduced by one over the square root of the number of inputs).

Figure 2 reveals more details about our fit. The top panel in this figure shows the values of  $\alpha_V(d/a)$  coming from

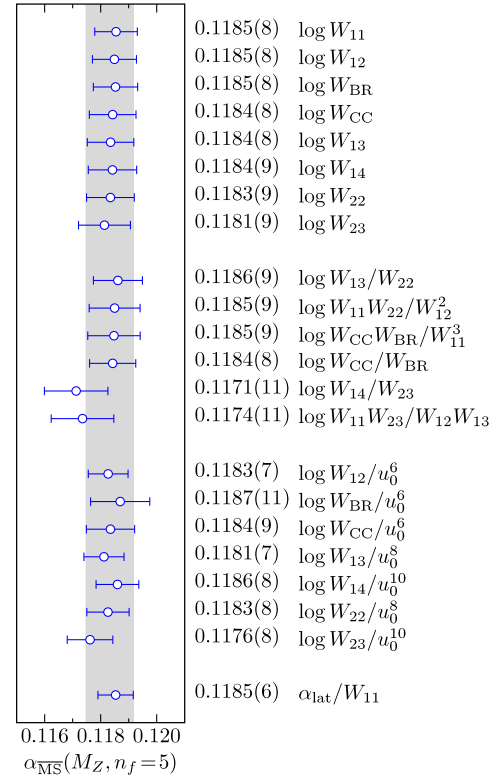


FIG. 1 (color online). Values for the 5-flavor  $\alpha_{\overline{\text{MS}}}$  at the Z-meson mass from each of 22 short-distance quantities. The gray band indicates our final result,  $0.1183(8)$ .  $\chi^2$  per data point is 0.2.

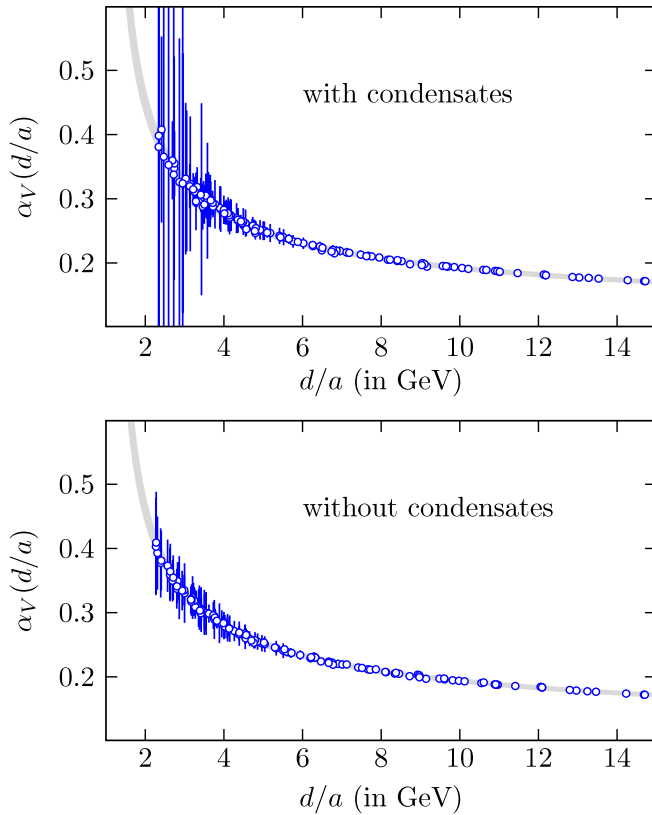


FIG. 2 (color online). Values for  $\alpha_V$  versus  $d/a$  from each short-distance quantity at each lattice spacing, with and without corrections for gluon condensates. The gray band shows the prediction from QCD evolution [Eq. (5)] assuming our composite fit value [Eq. (28)].

every short-distance quantity for every lattice spacing in our configuration sets. The  $\alpha_V$ s plotted here were obtained by refitting each piece of simulation data separately, rather than fitting results from all lattice spacings simultaneously as above. In these fits we used the values for  $c_n$  with  $n > 3$ ,  $w_m^{(1)}$ , etc. obtained from our simultaneous fit to all lattice spacings [21], which is why the individual data points align well with the perturbative result for  $\alpha_V(d/a)$  (the gray band). The fact that different points align so well is an indication of the self-consistency of our perturbative analysis across all scales and for all quantities. The size of the error bars for different points is determined by the perturbative and nonperturbative uncertainties associated with each piece of simulation data. Points with error bars much larger than the uncertainties in the perturbative  $\alpha_V$  (that is, much larger than the vertical width of the gray band) have little impact on our overall fits. The bulk of the uncertainty at low momentum comes from uncertainties in the gluon condensates. This is obvious when the results are reanalyzed without corrections for the condensates (bottom panel in Fig. 2). The most important simulation data is at large  $d/a$ , where errors are smaller than the plot points whether or not condensates are included.

It is useful to separate our error estimates into component pieces. The error estimate produced by our fitting code for a quantity like  $\alpha_{\overline{\text{MS}}}$  is approximately linear in all the variances  $\sigma^2$  that appear in the  $\chi^2$  function:

$$\sigma_{\alpha_{\overline{\text{MS}}}}^2 \approx \sum_{i=1}^{12} c_{Y_i} \sigma_{Y_i}^2 + \sum_{n=1}^{10} c_{c_n} \sigma_{c_n}^2 + c_{y_m^{(1)}} \sigma_{y_m^{(1)}}^2 + c_{r_{1m}^{(1)}} \sigma_{r_{1m}^{(1)}}^2 + c_{r_{1a}^{(2)}} \sigma_{r_{1a}^{(2)}}^2 + \dots \quad (29)$$

This works when errors are small, as they are here. To isolate the part of the total error that is associated with the statistical uncertainties in the  $Y_i$ , for example, the fit is rerun but with the corresponding variances rescaled by a factor  $f$  close to one ( $f = 1.01$ , for example):

$$\sigma_{Y_i}^2 \rightarrow f \sigma_{Y_i}^2 \quad (30)$$

for  $i = 1 \dots 12$ . Then

$$\frac{\sigma_{\alpha_{\overline{\text{MS}}}}^2(f) - \sigma_{\alpha_{\overline{\text{MS}}}}^2(f=1)}{f-1} \approx \sum_{i=1}^{12} c_{Y_i} \sigma_{Y_i}^2. \quad (31)$$

The square root of this quantity is the part of the total error due to the statistical uncertainties in the  $Y_i$ . This procedure can be repeated for each prior or group of priors that contributes to the  $\chi^2$  function. The sum of the variances obtained in this way for each part of the total error should equal  $\sigma_{\alpha_{\overline{\text{MS}}}}^2$ ; if it does not, errors may not be sufficiently small to justify the linear approximation in Eq. (29) [22].

In Table IV we present error budgets computed in this fashion for a sample of our determinations of  $\alpha_{\overline{\text{MS}}}(M_Z)$ . This table shows that our largest errors come from uncertainties in the perturbative coefficients with  $n \geq 4$ , statistical errors in the simulation values for  $(r_1/a)_i$ , systematic uncertainties in the physical value for  $r_1$ , and finite- $a$  lattice errors in  $r_1$ . Uncertainties in the parameters used to convert  $\alpha_0 = \alpha_V(7.5 \text{ GeV}, n_f = 3)$  into  $\alpha_{\overline{\text{MS}}}(M_Z, n_f = 5)$  have negligible impact. Also negligible are uncertainties due to the gluon condensate and statistical errors in the Wilson loops.

Our errors are greatly reduced because we can bound the size of perturbative coefficients  $c_n$  for  $n = 4$  and beyond. This is possible because we are fitting simulation data from six different lattice spacings simultaneously. As noted in [1], the  $n = 4$  coefficients are large, particularly for  $\log(W)$ s where typically our fits imply  $c_4/c_1 \approx -4(2)$ . As expected, perturbative higher-order coefficients are smaller for other quantities: for example, we find typically  $c_4/c_1 \approx -2(2)$  for tadpole-improved loops. The fit results for  $c_4/c_1$  and  $c_5/c_1$  for each of our short-distance quantities are given in Table I.

We tested the stability of our analysis procedure in several ways:

- (i) *Discarding simulation data:* Dropping data for any one of the lattice spacings gives results that are

TABLE IV. Sources of uncertainties in determinations of  $\alpha_{\overline{\text{MS}}}(M_Z, n_f = 5)$  from various short-distance quantities. Uncertainties are given as percentages of the final result in each case.

	$\log W_{11}$	$\log W_{12}$	$\log W_{22}$	$\log W_{11} W_{22}/W_{12}^2$	$\log W_{12}/u_0^6$	$\log W_{22}/u_0^8$	$\alpha_{\text{lat}}/W_{11}$
$c_1 \dots c_3$	0.1%	0.1%	0.1%	0.3%	0.1%	0.1%	0.1%
$c_n$ for $n \geq 4$	0.2	0.3	0.3	0.4	0.3	0.4	0.3
$am_q, r_1 m_q$ extrapolation	0.1	0.1	0.0	0.1	0.1	0.1	0.0
$(a/r_1)^2$ extrapolation	0.2	0.3	0.4	0.3	0.2	0.2	0.0
$(r_1/a)_i$ errors	0.4	0.4	0.4	0.3	0.3	0.3	0.3
$r_1$ errors	0.3	0.3	0.3	0.3	0.3	0.3	0.3
Gluon condensate	0.1	0.1	0.1	0.2	0.1	0.1	0.1
Statistical errors	0.0	0.0	0.0	0.1	0.0	0.0	0.0
$V \rightarrow \overline{\text{MS}} \rightarrow M_Z$	0.1	0.1	0.1	0.1	0.1	0.1	0.1
Total	0.6%	0.6%	0.7%	0.7%	0.6%	0.6%	0.5%

almost identical to our final result: the value of  $\alpha_{\overline{\text{MS}}}(M_Z)$  varies by no more than 0.12% from our final result, and its uncertainty ranges between 0.00083 and 0.00093. Dropping the two smallest lattice spacings, which are the most important, shifts  $\alpha_{\overline{\text{MS}}}(M_Z)$  to 0.1176(14). Keeping just the four, three, and two smallest lattice spacings gives 0.1183(9), 0.1180(10), and 0.1179(10), respectively (for sets 4–12, 7–12, and 9–12).

- (ii) *Perturbation theory scale changes:* Our results do not depend strongly on the choice of scale  $d/a$  used in the perturbation theory for each quantity. Reexpanding our perturbation theory for  $d \rightarrow d/1.5$  or  $d \rightarrow 1.5d$ , for example, shifts the overall  $\alpha_{\overline{\text{MS}}}(M_Z)$  to 0.1181(8) or 0.1184(8), respectively [23].
- (iii)  *$\overline{\text{MS}}$  throughout:* Reexpressing the perturbation theory for each quantity in terms of  $\alpha_{\overline{\text{MS}}}$  in place of  $\alpha_V$  gives almost the same overall results, 0.1185(10), but leads to significantly larger high-order coefficients in perturbation theory (2.5 times larger for small loops), somewhat greater dispersion between results from different quantities ( $\chi^2/22$  of 0.5 instead of 0.2), and larger uncertainties in the results from most quantities. The scale-setting procedure used to select the  $d$ s is tailored specifically for  $\alpha_V$  expansions; this is reflected by these results.
- (iv) *Adding more/fewer perturbative terms:* We allow terms up through tenth order in the perturbative expansions for the various short-distance quantities. Adding further terms has no impact on our results. Restricting perturbation theory to only fourth or fifth order also leaves our final result unchanged. Fitting is impossible with fewer than four terms: with three terms fits for individual Wilson loops, for example, to data from all 12 configuration sets are poor, with  $\chi^2/12$  becoming as large as 1.9 (rather than 0.4); and the couplings coming from the 22 different short-distance quantities disagree with each other, giving  $\chi^2/22 = 1.45$  (rather than 0.16).

- (v) *Adding more/fewer nonperturbative terms:* Adding higher-order terms in the chiral expansion in sea-quark masses [Eq. (12)] or further terms in the gluon-condensate expansion [Eq. (15)] does not change our final result at all. Omitting all corrections for the gluon condensates increases  $\alpha_{\overline{\text{MS}}}(M_Z)$  by two thirds of a standard deviation, to 0.1189(7). If we keep only the three smallest lattice spacings, which are the least sensitive to nonperturbative effects, we get 0.1180(10) whether or not the gluon condensates are included. We cannot fit all of our simulation data if we omit the chiral correction. Fitting without chiral corrections becomes possible if we keep only the subset of our data with  $m_{u/d}/m_s \approx 0.2$  (sets 2, 5, 7, 10, and 12); this gives  $\alpha_{\overline{\text{MS}}}(M_Z) = 0.1181(9)$ . (Our fit to  $\log(W_{11})$  gives

$$w_m^{(1)} = -0.18(6), \quad r_{1m}^{(1)} = -0.08(8), \quad (32)$$

which is typical of the other fits.)

Each of the variations examined here gives results that agree with our final result to within a standard deviation, suggesting that we have not underestimated the uncertainty in our result.

Our new result is one standard deviation above our previous result from Wilson loops [1],  $\alpha_{\overline{\text{MS}}}(M_Z) = 0.1170(12)$ , and has an error that is 33% smaller. Our new analysis differs in two important ways from our earlier work. First we include more lattice spacings, including one that is 50% smaller than the smallest we used before. (We used only configuration sets 1, 5, and 7 before.) This significantly reduces the errors. Second we now use more accurate values for  $r_1/a$ . These reduce uncertainties in the ratios of lattice spacings from different configuration sets, to a third of what they were in our earlier analysis. This matters since comparing results at different lattice spacings bounds the uncalculated high-order perturbation theory coefficients in our analysis ( $c_n$  for  $n \geq 4$ ). We are also allowing for larger finite- $a$  errors in  $r_1/a$  on the coarsest lattices than we did previously. The changes in  $r_1/a$ ,

together with the smaller lattice spacing, account for most of the increase in our final result.

Another change, which has less impact, is the inclusion of possible higher-dimension condensates. We also now do a more systematic analysis of effects due to the sea-quark mass, fitting results with many different masses, but the effect on our final result is small. Finally, we now use better scales  $d/a$  for the Creutz ratios and tadpole-improved loops than in our previous analysis [9]. Using the new scales shifts our final result up by only a third of a standard deviation, but the dispersion between results from different short-distance quantities is decreased from  $\chi^2/22 = 0.6$  to 0.2.

## VI. CONCLUSIONS

Any high-precision determination of  $\alpha_s$ , based upon lattice QCD simulations has to address several key issues:

- (i) *Finite-lattice-spacing errors:* Errors due to the finite lattice-spacing can enter in two ways. First they affect lattice determinations of the physical quantity or quantities used to set the scale of the coupling. In our analysis we use simulation values for  $r_1/a$ , from the static-quark potential, to determine ratios of scales from different configuration sets, and simulation values for the  $Y' - Y$  mass difference to set the overall scale [12]. In each case we use data from multiple lattice spacings to bound finite- $a$  errors, which are small because we use highly improved discretizations in our simulations. The second source of finite- $a$  errors, for some analyses (but not ours), is the lattice determination of the short-distance quantity that is compared with perturbation theory (to extract  $\alpha_s$ ). A short-distance quantity that is defined in continuum QCD—for example, changes  $V(r_a) - V(r_b)$  in the static-quark potential for small  $rs$  [1,8], or current-current correlators for  $c$ -quark currents [24]—will have finite- $a$  errors that must be included in the final error analysis. The use of multiple lattice spacings is again important. This is not an issue for us here because we analyze our short-distance quantities using lattice QCD perturbation theory, which treats finite- $a$  effects exactly (that is, to all orders in  $a$ , order by order in  $\alpha_V$ ). Both the simulation results and the perturbation theory for our 22 short-distance quantities are free of finite- $a$  errors. This greatly facilitates our use of results from multiple lattice spacings to bound uncalculated higher-order terms from perturbation theory.
- (ii) *Truncation errors from perturbation theory:* The coupling is determined by comparing perturbation theory with (nonperturbative) simulation results for a short-distance quantity. Generally the perturbation theory is known through only a few low orders in  $\alpha_s$ . The error analysis for any determination of the coupling must account for the uncalculated (but

certainly present) terms from higher-order perturbation theory. We not only account for the possibility of higher-order terms (through tenth order), using our Bayesian priors, but also attempt to estimate the size of these corrections by comparing values of our short-distance quantities at five different momentum scales  $d/a$ , corresponding to our five lattice spacings. We find sizable contributions from high-order terms, particularly for  $\log(W)$ s: leaving them out would shift our final result for the coupling down by one to two standard deviations (and lead to poor fits for most of our short-distance quantities). The agreement between our 22 different short-distance quantities, some with very different perturbative expansions (see Sec. II), is important evidence that we have analyzed truncation errors correctly.

- (iii) *Sea-quark vacuum polarization:* In our previous analysis [1], we showed that the coupling is quite sensitive to contributions from the vacuum polarization of sea quarks:  $\alpha_{\overline{\text{MS}}}(M_Z)$  is 30% smaller when all quark vacuum polarization is omitted. It is therefore important to include vacuum polarization from all three light quarks. Vacuum polarization corrections from heavy quarks ( $c$ ,  $b$ , and  $t$ ) can be computed using perturbation theory, but light quarks ( $u$ ,  $d$ , and  $s$ ) can only be incorporated non-perturbatively. In the past we have used simulations with fewer than three light quarks and extrapolated to  $n_f = 3$  ( $1/\alpha_{\overline{\text{MS}}}(M_Z)$  appears to be reasonably linear in  $n_f$ ) [25]. Here (and in our earlier paper [1]) contributions from all three light quarks are included in the configurations provided to us by the MILC collaboration. We also account for the small but (barely) measurable dependence upon the sea-quark masses.
- (iv) *Other lattice and nonperturbative artifacts:* Usually one must worry about the finite volume of the lattice in a QCD simulation. Our Wilson loops, however, are about as ultraviolet singular as is possible on a lattice, and so are completely insensitive to the volumes of our lattices (2.5 fm across). Another issue, for continuum as well as lattice determinations of the coupling, is the possibility of nonperturbative contributions to the short-distance quantity. Our quantities are sufficiently short-distance that we do not expect appreciable nonperturbative contamination. We nevertheless allowed for nonperturbative contributions from both gluons and quarks. The expected size of nonperturbative contributions varies widely over our set of 22 different short-distance quantities and 6 different lattice spacings. The excellent agreement among all of our results is strong evidence that we understand these systematic errors.

In this (and our previous) paper, we have addressed all of these issues. We have extended our earlier analysis of the strong coupling constant from Wilson loops in lattice QCD (and hadronic spectroscopy) to include results from 22 different short-distance quantities computed on 12 different lattices, with 6 distinct lattice spacings and a variety of sea-quark masses. We extracted a new value for the QCD coupling by comparing these  $22 \times 12 = 264$  different pieces of simulation data, varying by a factor of seven in momentum scales ( $d/a$  from 2.1 to 14.7 GeV), with perturbation theory. Our result,  $\alpha_{\overline{\text{MS}}}(M_Z, n_f = 5) = 0.1183(8)$ , is in excellent agreement with our previous result from Wilson loops [1], 0.1170 (12), and also with nonlattice determinations: for example, the world averages 0.1176 (20) from [26] and 0.1189 (10) from [27]. Our new result also agrees well with our very recent result, 0.1174 (12), from current-current correlators computed using lattice QCD [24].

While they are derived from the Wilson loops, our Creutz ratios and tadpole-improved loops provide coupling-constant information that is independent from that coming from the loops directly. This is because the highly ultraviolet contributions that dominate the loops largely cancel in the other quantities, making the latter more infrared. Consequently both perturbative and non-perturbative behavior differs significantly from quantity to quantity. This is particularly true of the sensitivity to non-perturbative contributions: for example, our most infrared Creutz ratios are more than 100 times more sensitive to gluon condensates than our most ultraviolet loops. That all of our quantities agree on the coupling (Fig. 1) is strong

evidence that we understand the systematic errors involved.

The close agreement of our results with nonlattice determinations of the coupling is a compelling quantitative demonstration that the perturbative QCD of jets, and the QCD of lattice simulations, which encompass both perturbative and nonperturbative phenomena, are the same theory. It is also further evidence that the simulation methods we use are valid. While early concerns about the light-quark discretization used here have been largely addressed [28,29], it remains important to test the simulation technology of lattice QCD at increasing levels of precision given the critical importance of lattice results for phenomenology [30].

## ACKNOWLEDGMENTS

We thank K. Maltman for discussions and comments. This work was supported by NSERC (Canada), STFC (UK), the NSF and DOE (USA), the Leverhulme Trust, and by SciDAC/US Lattice QCD Collaboration allocations at Fermilab. Results for the smallest lattice spacing required resources from the Argonne Leadership Computing Facility at Argonne National Laboratory, which is supported by the Office of Science of the U.S. Department of Energy under Contract No. DE-AC02-06CH11357. We also acknowledge the use of Chroma for part of our analysis [31]; and we thank Steve Gottlieb, Doug Toussaint, and their collaborators in the MILC collaboration for the use of their gluon configurations and for unpublished values of  $r_1/a$ .

- 
- [1] Q. Mason *et al.* (HPQCD Collaboration), Phys. Rev. Lett. **95**, 052002 (2005).
- [2] C. T. H. Davies *et al.* (HPQCD Collaboration), Phys. Rev. Lett. **92**, 022001 (2004).
- [3] G. P. Lepage and P. B. Mackenzie, Phys. Rev. D **48**, 2250 (1993).
- [4] S. J. Brodsky, G. P. Lepage, and P. B. Mackenzie, Phys. Rev. D **28**, 228 (1983).
- [5] We incorporate the  $c$  and  $b$  quarks using formulas from K. G. Chetyrkin, B. A. Kniehl, and M. Steinhauser, Phys. Rev. Lett. **79**, 2184 (1997) with quark masses of  $m_c(m_c) = 1.268(9)$  GeV from Allison *et al.* (2008), and  $m_b(m_b) = 4.18(4)$  GeV from the HPQCD Collaboration, in preparation (2008). For masses, see also J. H. Kühn, M. Steinhauser, and C. Sturm, Nucl. Phys. **B778**, 192 (2007).
- [6] Coupling  $\alpha_V(\mu)$  is defined in terms of  $\alpha_{\overline{\text{MS}}}(\bar{\mu})$ , where  $\bar{\mu} \equiv \mu \exp(-5/6)$  [3,4], using the static-quark potential. The potential has been computed through third order: Y. Schroder, Phys. Lett. B **447**, 321 (1999). Its expansion defines  $\alpha_V$  through order  $\alpha_{\overline{\text{MS}}}^3$ . Then  $\beta$ -function coefficients  $\beta_0$  through  $\beta_3$  for  $\alpha_V$  can be computed from the  $\beta$ -function coefficients for  $\alpha_{\overline{\text{MS}}}$ , which are given in T. van Ritbergen, J. A. M. Vermaseren, and S. A. Larin, Phys. Lett. B **400**, 379 (1997).
- [7] We are not yet able to update the analysis in our previous paper of the static-quark potential.
- [8] Q. Mason and H. Trotter (unpublished); Q. Mason, Ph.D. thesis, Cornell University, 2004.
- [9] The lowest-order procedure (from [3]) for setting scales sometimes gives scales that are misleadingly small. A simple test for this problem, together with a more robust procedure for setting scales, is presented in: K. Hornbostel, G. P. Lepage, and C. Morningstar, Phys. Rev. D **67**, 034023 (2003). The scales for most of the tadpole-improved loops (all but  $W_{13}$  and  $W_{14}$ ) and all of the Creutz ratios do not pass this test. For these cases, we have used the more robust procedure to obtain new scales, which we list in Table I. Consequently scales for these quantities differ from what we used in [1]. The resulting changes in our final results are not large since we are working to very high orders (and therefore scale changes have a small impact, as illustrated in Sec. V B).

- [10] In footnote [8] of [1] we erroneously said that the expansion for  $\alpha_V$  in terms of  $\alpha_{\overline{\text{MS}}}$  has no terms past third order. There and here, it is the beta function [Eq. (5)] that we define to have no terms beyond  $\beta_3$ . We thank K. Maltman for pointing out this inconsistency.
- [11] C. Aubin *et al.*, Phys. Rev. D **70**, 094505 (2004); MILC Collaboration (private communication).
- [12] A. Gray, I. Allison, C.T.H. Davies, E. Dalgic, G.P. Lepage, J. Shigemitsu, and M. Wingate (HPQCD Collaboration), Phys. Rev. D **72**, 094507 (2005). The value for  $r_1$  given in this paper has been extensively checked in many other calculations, some involving light quarks and others heavy quarks: see, for example, [2].
- [13] C. Aubin *et al.*, Phys. Rev. D **70**, 094505 (2004).
- [14] This is quite obvious from lattice QCD simulations. It is perhaps because sea-quark contributions are suppressed by  $1/N_c$ , where  $N_c = 3$  is the number of QCD colors, in a  $1/N_c$  expansion of QCD.
- [15] For a recent analysis of condensate values see B.L. Ioffe, Prog. Part. Nucl. Phys. **56**, 232 (2006).
- [16] The corrections that remove the gluon condensates from the Monte Carlo results for a Wilson loop introduce correlations into the covariance matrix for results from different lattice spacings. This is because the corrections for different lattice spacings are related to each other [by Eqs. (14) and (15)], where the condensate values are the same for different lattice spacings. It is important to include this correlation when fitting the dependence upon lattice spacing.
- [17] We thank K. Maltman for an extensive discussion about the role of condensates here.
- [18] Rather than approximating  $\alpha_V$  by a constant, we could put in the running coupling at a scale like  $1/a$ . In this case, however, it makes little difference to the final fits. Our analysis is not sufficiently accurate to resolve the difference between a constant and a running coupling in the  $a^2$  corrections.
- [19] G.P. Lepage, B. Clark, C.T.H. Davies, K. Hornbostel, P.B. Mackenzie, C. Morningstar, and H. Trottier, Nucl. Phys. B, Proc. Suppl. **106**, 12 (2002).
- [20] We average our 22 different results weighted by their inverse variances, giving more weight to results with smaller variances. The variance for our composite result is the inverse of the average of the inverse variances from the separate determinations.
- [21] Specifically we fit each single piece of simulation data separately using the fitting function described in Secs. IV and V but with priors taken from the means and standard deviations obtained for each parameter other than  $\alpha_0$  in our overall fits for each short-distance quantity at all lattice spacings. Fit parameter  $\alpha_0$  is effectively unconstrained by the prior in these individual fits since we use the same prior as in the overall fits (to multiple lattice spacings). Parameter  $\alpha_0$  is the main parameter adjusted by the individual fits.
- [22] Occasionally the difference in Eq. (31) comes out negative. This can be caused by instabilities in the fit, in which case a different choice of  $f$  might fix the problem. It can also be the case that a term enters Eq. (29) with a negative sign. In such cases we use the absolute value of Eq. (31) for the partial variance.
- [23] The following paper, which was posted after the initial version of our paper, reanalyzes some of our Monte Carlo data using a different reorganization of perturbation theory. Results from that paper agree to within a standard deviation with our results. K. Maltman, D. Leinweber, P. Moran, and A. Sternbeck, arXiv:0807.2020 [Phys. Rev. D (to be published)].
- [24] I. Allison *et al.*, Phys. Rev. D **78**, 054513 (2008).
- [25] C.T.H. Davies, K. Hornbostel, G.P. Lepage, P. McCallum, J. Shigemitsu, and J.H. Sloan, Phys. Rev. D **56**, 2755 (1997). This paper found  $\alpha_{\overline{\text{MS}}}(M_Z) = 0.1174(24)$  by extrapolating from data with  $n_f = 0$  and  $n_f = 2$ .
- [26] A world average of 0.1176(20) is given in W.-M. Yao *et al.* (Particle Data Group), J. Phys. G **33**, 1 (2006).
- [27] A world average of 0.1189(10) is given in S. Bethke, Prog. Part. Nucl. Phys. **58**, 351 (2007).
- [28] S.R. Sharpe, Proc. Sci., LAT2006 (2006) 022 [arXiv:hep-lat/0610094].
- [29] C. Bernard, M. Golterman, Y. Shamir, and S.R. Sharpe, Phys. Rev. D **77**, 114504 (2008).
- [30] The main formal concern about staggered quarks lies in the use of the fourth-root of the staggered-fermion determinant to remove redundant tastes from the theory. Errors connected with this approximation vanish with the lattice spacing, and therefore uncertainties in our final results due to this approximation are included in our estimates of the uncertainties due to the  $am_q$  and  $(a/r_1)^2$  extrapolations (Table IV).
- [31] R.G. Edwards and B. Joo (SciDAC Collaboration and LHPC Collaboration, and UKQCD Collaboration), Nucl. Phys. B, Proc. Suppl. **140**, 832 (2005).